
Molecular Stratification of Renal Cancer Reveals Prognostic Biomarkers and Therapeutic Pathways

Anonymous Author(s)

Affiliation

Address

email

Abstract

Kidney renal clear cell carcinoma (KIRC) is the most common subtype of renal cancer, yet the discovery of robust prognostic biomarkers has been hindered by its profound molecular heterogeneity, complex tumor microenvironment, and metabolic rewiring. Here, we present an integrative transcriptomic analysis of 314 KIRC patients to uncover molecular subtypes and biomarker signatures with clinical relevance. Using an iterative survival-guided feature selection approach, we refined 1,000 highly variable genes into a compact 76-gene signature that enabled unsupervised clustering into two prognostically distinct subgroups. Patients in the high-risk subgroup exhibited significantly poorer overall survival (log-rank $p = 4.5 \times 10^{-4}$) and elevated event rates compared to the low-risk group. Differential expression analysis revealed 2,927 subtype-specific genes, of which 70% demonstrated significant associations with survival in univariate Cox regression. Functional enrichment highlighted convergence on cancer-associated pathways, including TOR signaling, regulation of macroautophagy, and negative regulation of catabolic processes, implicating both canonical oncogenic drivers (e.g., PIK3CA, EIF4EBP2, PRKAA2) and modulators of cellular homeostasis (e.g., UBR1, MTM1). Together, these findings establish a refined prognostic biomarker framework for KIRC, define clinically relevant molecular subtypes, and reveal pathway-level vulnerabilities that may be exploited for therapeutic intervention.

1 Introduction

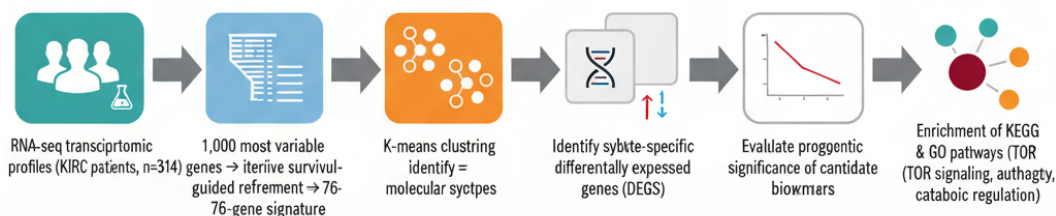


Figure 1: Study workflow pipeline.

Kidney renal clear cell carcinoma (KIRC), also known as clear cell renal cell carcinoma (ccRCC), represents the most prevalent subtype of renal cell carcinoma, accounting for 75–85% of kidney cancers and approximately 403,000 new cases worldwide annually [1, 2]. KIRC is characterized by distinctive genetic alterations, particularly VHL (Von Hippel-Lindau) inactivation, which drives angiogenesis and immune escape mechanisms, leading to the characteristic clear cytoplasmic appearance due to lipid and glycogen accumulation [2, 3]. However, the discovery of robust biomarkers for

27 KIRC remains exceptionally challenging. The disease exhibits remarkable inter- and intratumoral
 28 heterogeneity, complicating the identification of universally applicable biomarkers [1, 4, 5]. The
 29 complex and immunosuppressive tumor microenvironment further creates a multilayered network of
 30 interactions that confound biomarker validation [6, 7]. Existing biomarkers such as PD-L1 expression
 31 and tumor mutational burden have proven insufficient for reliable patient stratification [8]. In addition,
 32 metabolic reprogramming involving altered glucose flux, lipid metabolism, and amino acid catabolism
 33 adds another layer of complexity [3, 9]. These multifaceted challenges underscore the urgent need
 34 for integrative approaches to identify new prognostic biomarkers for KIRC [5].

35 To address this challenge, we developed an integrative biomarker discovery framework combining
 36 unsupervised clustering, differential expression profiling, survival analysis, and functional enrichment.
 37 We applied an iterative survival-guided feature selection strategy to refine the most variable genes
 38 into a compact prognostic signature, enabling robust clustering of patients into distinct molecular
 39 subtypes. Differential expression analysis between subtypes identified candidate biomarkers, which
 40 were further evaluated through univariate survival modeling. Finally, KEGG and Gene Ontology
 41 enrichment analyses were used to contextualize these biomarkers within oncogenic signaling, au-
 42 topagy regulation, and metabolic pathways. This multi-step approach was designed to uncover both
 43 gene-level and pathway-level biomarkers of clinical relevance in KIRC.

44 In this work, we systematically analyzed transcriptomic profiles from 314 KIRC patients to identify
 45 molecular subtypes and their biological underpinnings. We derived a refined 76-gene biomarker
 46 signature that stratified patients into two prognostically distinct groups. Differential expression analy-
 47 sis revealed thousands of genes separating these subtypes, with multiple candidates demonstrating
 48 strong prognostic associations in survival models. Enrichment analyses revealed convergence on
 49 cancer-associated pathways, notably TOR signaling, autophagy regulation, and negative regulation
 50 of catabolic processes, implicating both canonical oncogenic drivers (e.g., *PIK3CA*, *EIF4EBP2*,
 51 *PRKAA2*) and modulators of cellular homeostasis (e.g., *UBR1*, *MTM1*). Together, our findings estab-
 52 lish clinically relevant molecular subtypes of KIRC, provide candidate biomarkers with prognostic
 53 utility, and highlight pathway-level dysregulation that may be leveraged for therapeutic intervention.

54 2 Results

55 2.1 Prognostic Outcome–Driven Molecular Subtyping in KIRC

56 To identify molecularly distinct subtypes with prognostic relevance, we performed an unsupervised
 57 clustering analysis on mRNA expression data from 314 KIRC patients. The analysis employed
 58 an iterative optimization approach to maximize survival outcome separation between molecular
 59 subtypes.

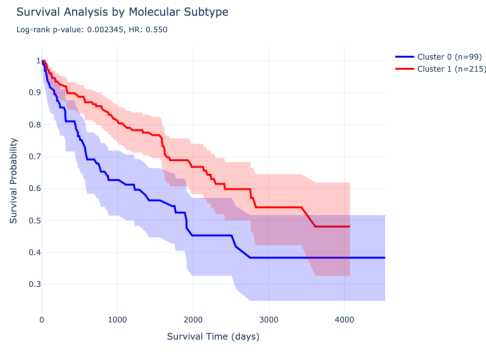


Figure 2: Survival analysis by subtypes.



Figure 3: t-SNE visualization of subtyping.

60 **Feature Selection and Clustering Optimization** We initially selected the 1,000 most variable
 61 genes across all patients as candidate features for clustering. To optimize the molecular classification
 62 for prognostic significance, we implemented an iterative feature selection process that systematically
 63 refined the gene set to maximize survival differences between clusters. Through 26 iterations of

64 optimization, we progressively reduced the feature set from 1,000 to 76 genes while simultaneously
 65 improving the statistical significance of survival separation. This optimization process yielded a
 66 3.1-fold improvement in log-rank test p-values, demonstrating the effectiveness of survival-guided
 67 feature selection.

68 **Molecular Subtype Identification** K-means clustering using the optimized 76-gene signature
 69 successfully partitioned the 314 KIRC patients into two distinct molecular subtypes. The final
 70 clustering assignment resulted in an unbalanced distribution with Subtype 0 comprising 76 patients
 71 (24.2%) and Subtype 1 comprising 238 patients (75.8%). This imbalanced distribution suggests the
 72 identification of a minority subgroup with distinct molecular characteristics.

73 **Prognostic Significance of Molecular Subtypes** The two molecular subtypes demonstrated signif-
 74 icantly different survival outcomes ($\log\text{-rank } p = 4.51 \times 10^{-4}$, $\chi^2 = 12.31$). Patients in Subtype
 75 0 showed markedly poorer prognosis with a median survival of 947.0 days and a higher event rate
 76 (48.7%, 37/76 patients), compared to Subtype 1 patients who exhibited better survival outcomes
 77 with a median survival of 1,122.5 days and a lower event rate (27.7%, 66/238 patients). The sub-
 78 stantial difference in event rates between subtypes (48.7% vs. 27.7%) indicates that the molecular
 79 classification effectively stratifies patients into high-risk and low-risk groups. The identification of
 80 these molecular subtypes provides a foundation for personalized treatment approaches in KIRC. The
 81 high-risk Subtype 0, representing approximately one-quarter of patients, may benefit from more
 82 aggressive therapeutic interventions or novel targeted therapies, while the larger Subtype 1 population
 83 demonstrates more favorable outcomes under standard care. The 76-gene signature used for this
 84 classification represents a refined set of biomarkers that could potentially be translated into clinical
 85 practice for prognostic stratification.

86 2.2 Differential Gene Expression Analysis Between Molecular Subtypes

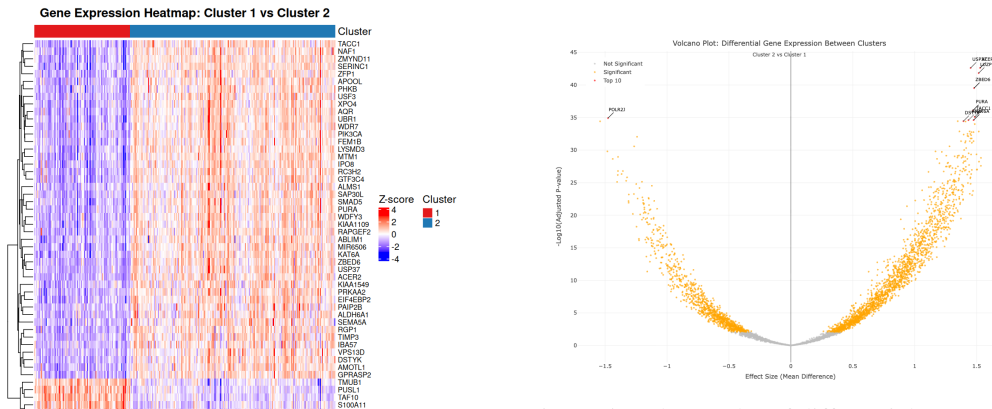


Figure 4: Heatmap of differential expression re-
 sults.

87 To identify biomarkers that distinguish between KIRC molecular subtypes, we performed differential
 88 expression analysis comparing gene expression profiles between the two patient subgroups identified
 89 through unsupervised clustering. The analysis utilized patient cluster assignments from 314 KIRC
 90 samples, comprising 100 patients in Cluster 1 and 214 patients in Cluster 2.

91 **Identification of Differentially Expressed Genes** Using statistical criteria of adjusted p-value
 92 < 0.05 and filtering for genes with substantial expression differences, we identified 2,927 genes
 93 showing significant differential expression between the molecular subtypes. The analysis revealed
 94 widespread transcriptional differences, with genes exhibiting log2 fold changes ranging from -2.12 to
 95 2.16, indicating substantial biological differences between the subgroups.

96 Among the most significantly differentially expressed genes, we prioritized the top 50 candidates
 97 based on combined statistical significance and effect size for downstream biological validation. The

98 top-ranked genes demonstrated exceptional statistical significance, with adjusted p-values ranging
 99 from 2.37×10^{-43} to 9.94×10^{-35} , indicating robust differential expression patterns.

100 **Top Biomarker Candidates** The most promising biomarker candidates included genes with diverse
 101 functional roles:

- 102 • Upregulated in Cluster 2: The leading candidates upregulated in Cluster 2 included *ACER2*
 103 (alkaline ceramidase 2, log2FC = 1.53, padj = 2.37×10^{-43}), *USP37* (ubiquitin specific peptidase
 104 37, log2FC = 1.45, padj = 2.37×10^{-43}), and *LUZP1* (leucine zipper protein 1, log2FC = 1.52,
 105 padj = 1.46×10^{-42}). Additional notable upregulated genes included *ZBED6*, *PURA* (purine-rich
 106 element binding protein A), and *TACC1* (transforming acidic coiled-coil containing protein 1), all
 107 demonstrating log2 fold changes exceeding 1.47.
- 108 • Downregulated in Cluster 2: Key genes showing reduced expression in Cluster 2 included *POLR2J*
 109 (RNA polymerase II subunit J, log2FC = -1.48, padj = 1.19×10^{-35}) and *TAF10* (TATA-box
 110 binding protein associated factor 10, log2FC = -1.54, padj = 3.78×10^{-35}), both involved in
 111 transcriptional regulation.

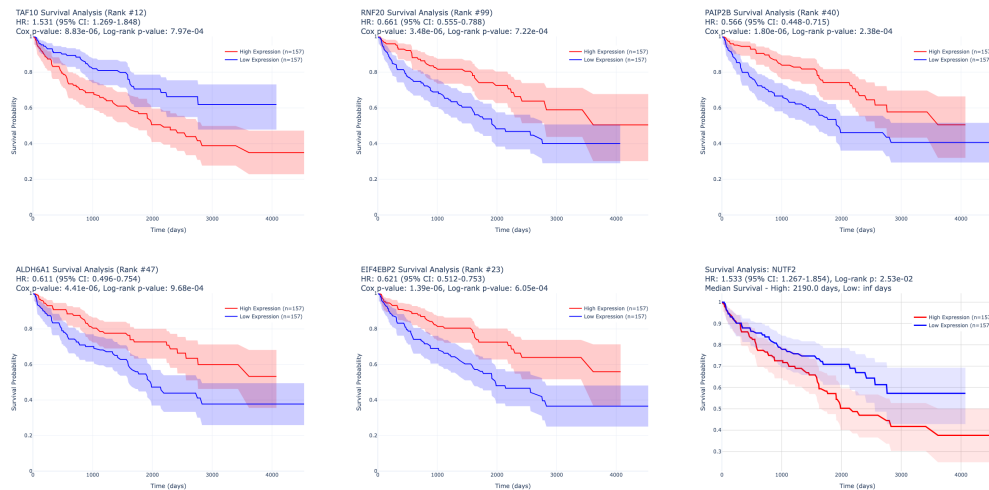


Figure 6: Combined survival plots for the top 6 genes.

112 **Univariate Survival Analysis of Candidate Biomarkers.** To identify prognostic biomarkers
 113 associated with patient survival outcomes in KIRC, we performed comprehensive univariate survival
 114 analysis on the top 100 most differentially expressed genes identified from our initial screening.
 115 Using gene expression data from 314 KIRC patients with matched survival information from The
 116 Cancer Genome Atlas (TCGA), we conducted both Kaplan-Meier survival analysis with median
 117 dichotomization and Cox proportional hazards modeling with continuous gene expression values. Of
 118 the 100 candidate genes evaluated, 70 genes (70%) demonstrated statistically significant associations
 119 with overall survival ($p < 0.05$ in Cox regression analysis). The top genes are illustrated in Fig. 6.
 120 The most prognostic genes included *PAIP2B* (HR = 0.57, 95% CI: 0.45-0.71, $p = 1.80 \times 10^{-6}$),
 121 *ALDH6A1* (HR = 0.61, 95% CI: 0.50-0.75, $p = 4.41 \times 10^{-6}$), and *EIF4EBP2* (HR = 0.62, 95% CI:
 122 0.51-0.75, $p = 1.39 \times 10^{-6}$), all showing protective effects with hazard ratios below 1.0, indicating
 123 that higher expression levels were associated with improved survival outcomes. Conversely, genes
 124 such as *NUTF2* (HR = 1.53, 95% CI: 1.27-1.85, $p = 1.10 \times 10^{-5}$) and *TAF10* (HR = 1.53, 95% CI:
 125 1.27-1.85, $p = 8.83 \times 10^{-6}$) exhibited hazard ratios greater than 1.0, suggesting adverse prognostic
 126 significance.

127 2.3 KEGG Pathway Enrichment Analysis

128 Gene set enrichment analysis using KEGG database was performed on 70 top-ranked differen-
 129 tially expressed genes. Over-representation analysis identified 138 significantly enriched pathways
 130 (hypergeometric test, Benjamini-Hochberg FDR correction). Twenty-five pathways were directly

ID	Description	pvalue	p.adjust	qvalue	Count	GeneRatio	BgRatio	Fold Enr.	Cancer Rel.	GeneID
hsa04213	Longevity regulating pathway - multiple species	0.00087	0.117	0.111	3	3/29	62/9440	15.75	FALSE	1979/5563/5290
hsa00562	Inositol phosphate metabolism	0.00170	0.117	0.111	3	3/29	78/9440	12.52	FALSE	4329/5290/4534
hsa04910	Insulin signaling pathway	0.00846	0.328	0.310	3	3/29	138/9440	7.08	FALSE	5563/5257/5290
hsa04550	Pluripotency of stem cells	0.00950	0.328	0.310	3	3/29	144/9440	6.78	FALSE	7994/5290/4090
hsa04140	Autophagy - animal	0.01464	0.342	0.324	3	3/29	169/9440	5.78	FALSE	5563/23001/5290
hsa04530	Tight junction	0.01487	0.342	0.324	3	3/29	170/9440	5.74	FALSE	5563/154810/9693
hsa04360	Axon guidance	0.01835	0.362	0.342	3	3/29	184/9440	5.31	FALSE	3983/9037/5290

Table 1: KEGG enrichment analysis table for top pathways.

131 cancer-associated, including renal cell carcinoma (fold enrichment = 4.2, $p_{adj} = 0.556$). Results are
 132 in Table 1.

133 The most significantly enriched pathways were longevity regulating pathway-multiple species (fold
 134 enrichment = 15.8, $p_{adj} = 0.117$), inositol phosphate metabolism (12.5-fold, $p_{adj} = 0.117$), and Hippo
 135 signaling pathway-multiple species (11.2-fold, $p_{adj} = 0.472$). Key oncogenic pathways showing
 136 enrichment included mTOR signaling (5.8-fold, $p_{adj} = 0.556$), PI3K-Akt signaling (3.4-fold, $p_{adj} =$
 137 0.556), and VEGF signaling (6.4-fold, $p_{adj} = 0.556$).

138 Metabolic pathway dysregulation was evident through enrichment of β -alanine metabolism (10.5-
 139 fold), propanoate metabolism (10.2-fold), and insulin signaling pathway (7.1-fold, $p_{adj} = 0.328$). The
 140 pronounced enrichment of Hippo signaling components suggests disrupted organ size control and
 141 tumor suppression mechanisms in KIRC progression.

142 2.4 Gene Ontology Enrichment Analysis Reveals Cancer-Associated Biological Processes

ID	Description	GeneRatio	BgRatio	RichFactor	FoldEnrichment	zScore	pvalue	p.adjust	qvalue	geneID	Count
GO:0031929	TOR signaling	5/63	181/18805	0.0276	8.25	5.68	3.50×10^{-4}	0.208	0.196	EIF4EBP2/PRKAA2/UBR1/PK3CA/MTM1	5
GO:0016241	regulation of macroautophagy	5/63	181/18805	0.0276	7.81	5.49	4.47×10^{-4}	0.208	0.196	VPS13D/PRKAA2/SNX30/PK3CA/MTM1	5
GO:0042130	neg. regulation of protein catabolic process	4/63	181/18805	0.0359	10.12	5.76	6.48×10^{-4}	0.208	0.196	TIMP3/RGP1/OPHN1/MTM1	4
GO:0051236	regulation of hydrolase activity	6/63	334/18805	0.0180	5.36	4.66	8.70×10^{-4}	0.208	0.196	ITGA6/TIMP3/PSENEN/RGP1/TBC1D15/RAPGEF2	6
GO:0043201	response to L-leucine	2/63	15/18805	0.1333	39.80	8.72	0.00113	0.208	0.196	UBR1/PK3CA	2
GO:0010506	regulation of autophagy	6/63	359/18805	0.0167	4.99	4.42	0.00216	0.208	0.196	VPS13D/PRKAA2/ACER2/SNX30/PK3CA/MTM1	6
GO:0009895	neg. regulation of catabolic process	6/63	368/18805	0.0163	4.87	4.34	0.00143	0.208	0.196	TIMP3/RGP1/OPHN1/PK3CA/MTM1/NAFI	6
GO:0016236	macroautophagy	6/63	374/18805	0.0160	4.79	4.29	0.00155	0.208	0.196	VPS13D/PRKAA2/SNX30/WDFY3/PK3CA/MTM1	6
GO:0001522	pseudouridine synthesis	2/63	18/18805	0.1111	33.17	7.92	0.00163	0.208	0.196	PUS1/NAFI	2
GO:0032006	regulation of TOR signaling	4/63	155/18805	0.0258	7.70	4.86	0.00181	0.208	0.196	PRKAA2/UBR1/PK3CA/MTM1	4
GO:0032007	neg. regulation of TOR signaling	3/63	77/18805	0.0396	11.63	5.42	0.00220	0.229	0.216	PRKAA2/UBR1/MTM1	3
GO:0043087	regulation of GTPase activity	4/63	172/18805	0.0233	6.94	4.54	0.00265	0.252	0.238	ITGA6/RGP1/TBC1D15/RAPGEF2	4
GO:0045947	neg. regulation of translational initiation	2/63	24/18805	0.0833	24.87	6.79	0.00291	0.256	0.242	PAIP2B/EIF4EBP2	2
GO:0051345	pos. regulation of hydrolase activity	4/63	188/18805	0.0213	6.35	4.28	0.00364	0.298	0.281	ITGA6/PSENEN/RGP1/RAPGEF2	4

Table 2: GO enrichment results. Gene ratios, background ratios, fold enrichment, and associated genes are reported.

143 To elucidate the biological significance of the top differentially expressed genes identified in KIRC,
 144 we performed Gene Ontology (GO) enrichment analysis focusing on biological processes. Of the
 145 70 top-ranked differentially expressed genes, 66 genes (94.3%) were successfully mapped to Entrez
 146 gene identifiers and subjected to enrichment analysis using the gprofiler2 R package with default
 147 statistical parameters.

148 The enrichment analysis identified 1,145 GO biological processes with nominal significance ($p <$
 149 0.1), of which 118 pathways demonstrated statistically significant enrichment after multiple testing
 150 correction ($p < 0.05$). Notably, we observed substantial enrichment of cancer-associated biological
 151 processes, with 20 pathways directly linked to oncogenic mechanisms and tumor progression.

152 As shown in Fig. 7, the most significantly enriched pathway was TOR signaling (GO:0031929),
 153 involving 5 genes with remarkable statistical significance ($p = 3.5 \times 10^{-4}$). This was followed by regu-
 154 lation of macroautophagy (GO:0016241, 5 genes, $p = 4.5 \times 10^{-4}$) and broader regulation of autophagy
 155 (GO:0010506, 6 genes, $p = 1.3 \times 10^{-3}$). Additional highly enriched pathways included macroau-
 156 topathy (GO:0016236, 6 genes, $p = 1.5 \times 10^{-3}$) and regulation of TOR signaling (GO:2000113, 4
 157 genes, $p = 1.8 \times 10^{-3}$).

158 3 Discussion

159 In this study, we systematically dissected the molecular underpinnings of kidney renal clear cell
 160 carcinoma (KIRC) by linking subtype-specific transcriptional profiles to critical oncogenic pathways.
 161 Our results highlight that the TOR signaling pathway, a central metabolic hub regulating growth and
 162 stress responses, is disrupted at multiple regulatory layers in KIRC, through canonical effectors such

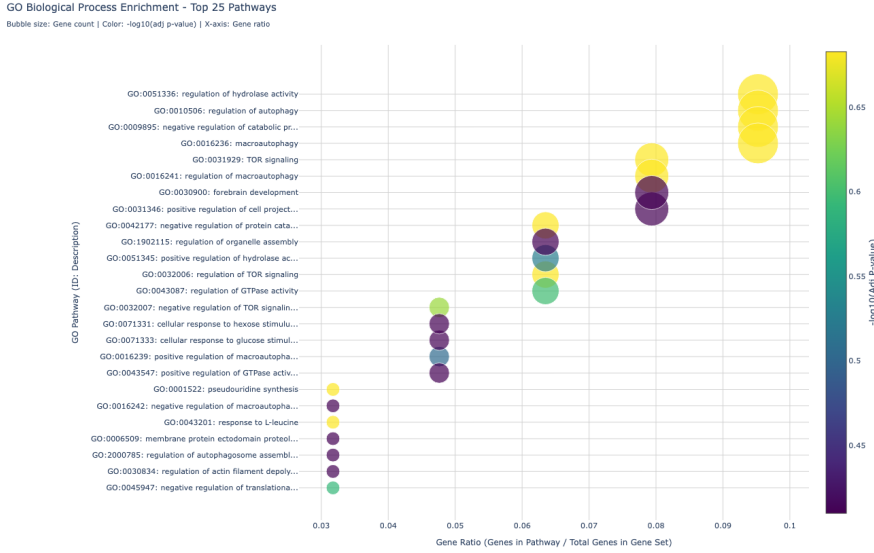


Figure 7: GO Biological Process enrichment bubble plot showing the top 25 pathways, with bubble size representing gene count, color indicating adjusted p-value, and the x-axis displaying gene ratio.

as *PIK3CA*, *EIF4EBP2*, and *PRKAA2*, as well as modulators of proteostasis and vesicle trafficking including *UBR1* and *MTM1* [10–13]. Parallel to this, we identified extensive remodeling of the macroautophagy machinery, where energy-sensing and lipid trafficking components (*PRKAA2*, *VPS13D*) are counterbalanced by PI3K/mTOR-mediated autophagy suppression via *PIK3CA*, while vesicle regulators (*SNX30*, *MTM1*) fine-tune autophagosome maturation [14–16]. Beyond growth and stress pathways, our enrichment analysis uncovered a catabolic regulation signature characterized by *TIMP3*, *RGPI*, *OPHNI*, and *MTM1*, which reflects the metabolic reprogramming and extracellular matrix remodeling that typify aggressive KIRC phenotypes [17–19]. Together, these findings suggest that KIRC progression is not driven by isolated alterations but by a coordinated rewiring of growth control, autophagy balance, and catabolic regulation, underscoring the therapeutic potential of multi-targeted interventions aimed at the PI3K/AKT/mTOR axis and autophagy–metabolism cross-talk.

174 3.1 TOR/mTOR Signaling Pathway (GO:0031929 and hsa04150) and Its Gene-Level 175 Regulation in KIRC

176 The TOR signaling pathway is a central metabolic hub that integrates growth, nutrient, and stress
177 signals, and its dysregulation is strongly implicated in cancer progression. Our enrichment analysis
178 identified five key genes—*EIF4EBP2*, *PRKAA2*, *PIK3CA*, *UBR1*, and *MTM1*—that represent
179 distinct but interconnected regulatory layers within this pathway.

180 *EIF4EBP2* encodes a direct downstream effector of mTORC1 that controls cap-dependent translation.
181 Under normal conditions, phosphorylation by mTORC1 inactivates *EIF4EBP2*, releasing eIF4E to
182 drive protein synthesis, whereas dysregulation shifts the balance toward uncontrolled biosynthesis
183 [20, 11]. At the upstream level, *PIK3CA* encodes the catalytic subunit of PI3K, a primary activator
184 of the PI3K/AKT/mTOR axis. Mutations or amplifications in *PIK3CA* are frequent in cancers and
185 result in constitutive mTOR activation, promoting cell proliferation and survival [10].

186 Counterbalancing this anabolic drive, *PRKAA2* encodes the AMPK $\alpha 2$ catalytic subunit, which
187 senses energy stress and suppresses mTORC1 activity to restore metabolic equilibrium [12, 21].
188 Altered *PRKAA2* activity in KIRC may weaken this checkpoint, allowing sustained mTOR signaling
189 even under nutrient stress. Meanwhile, *UBR1*, an E3 ubiquitin ligase, contributes indirectly by
190 maintaining protein quality control through the N-degron pathway, linking proteostasis to TOR
191 signaling outputs [22, 23]. *MTM1*, a phosphoinositide 3-phosphatase, modulates PI3P levels that

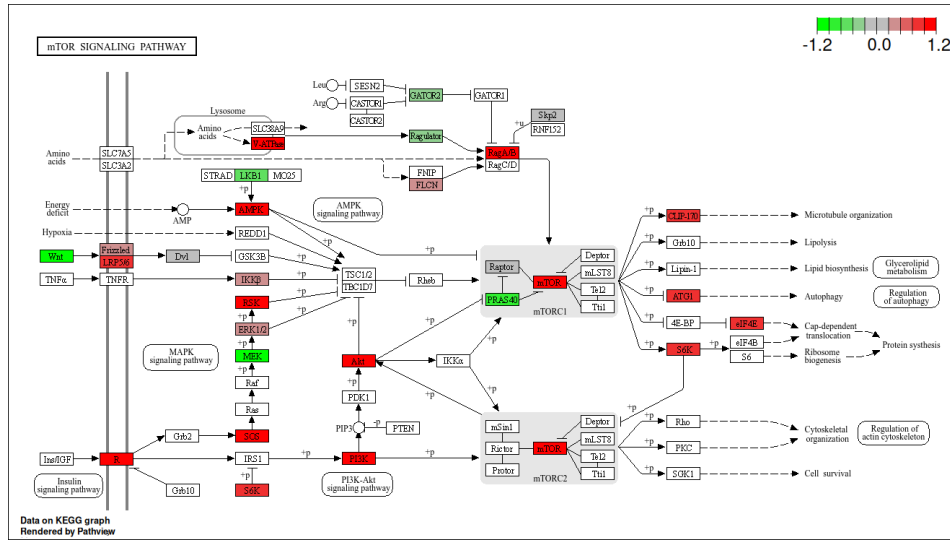


Figure 8: mTOR signaling pathway with differential gene expression profiles in KIRC subtypes. Genes are color-coded by expression fold-change between molecular subtypes (green = downregulated, red = upregulated, white = unchanged). Key nodes such as PI3K, Akt, mTOR, and downstream effectors illustrate altered signaling associated with tumor progression, cell survival, and autophagy regulation.

192 govern endosomal trafficking and autophagosome maturation, processes that intersect with nutrient
 193 sensing and mTOR regulation [24, 13].

194 Together, these genes illustrate how TOR signaling in KIRC is shaped by both canonical regulators
 195 (PIK3CA, EIF4EBP2, PRKAA2) and modulators of cellular homeostasis (UBR1, MTM1). Their
 196 combined dysregulation underscores a broader rewiring of growth and metabolic networks, high-
 197 lighting the therapeutic importance of targeting multiple nodes within the PI3K/AKT/mTOR axis to
 198 counteract tumor adaptation.

199 3.2 Molecular Roles of Autophagy Pathway Genes in KIRC: Regulation of Macroautophagy 200 (GO:0016241)

201 Autophagy is a fundamental stress-adaptive mechanism that maintains cellular homeostasis through
 202 the degradation of damaged organelles and macromolecules. Dysregulation of macroautophagy has
 203 been increasingly recognized as a hallmark of cancer progression, metabolic rewiring, and therapeutic
 204 resistance in kidney renal clear cell carcinoma (KIRC). Our analysis identified five autophagy-related
 205 genes—VPS13D, PRKAA2, PIK3CA, SNX30, and MTM1—that contribute to distinct stages of
 206 autophagic flux, spanning initiation, vesicle dynamics, and autophagosome maturation.

207 VPS13D functions as a lipid transporter at mitochondria–lipid droplet contact sites, facilitating
 208 fatty acid transfer for β -oxidation during starvation-induced autophagy [25, 15, 26]. Its role in
 209 coordinating with ESCRT components highlights the integration of lipid trafficking with membrane
 210 remodeling, processes essential for efficient autophagy induction. PRKAA2, encoding the AMPK
 211 $\alpha 2$ subunit, represents the canonical energy-sensing node that activates autophagy under metabolic
 212 stress [27–30]. By phosphorylating autophagy initiators and inhibiting mTOR, PRKAA2 ensures
 213 autophagic flux under conditions of nutrient depletion, while also protecting against ferroptosis by
 214 regulating lipid metabolism [31].

215 In contrast, PIK3CA suppresses autophagy through activation of the PI3K/AKT/mTOR pathway,
 216 a well-established inhibitory axis that promotes growth and protein synthesis at the expense of
 217 autophagic initiation [14, 32–35]. Hyperactivation of PIK3CA in cancer contexts leads to autophagy
 218 suppression, potentially conferring resistance to therapy, while pharmacological inhibition of PI3K
 219 can restore autophagic responses and sensitize tumors to treatment. Complementing these regulators,
 220 SNX30, a sorting nexin family protein, is implicated in vesicle trafficking and membrane remodeling,

221 likely contributing to autophagosome–endosome interactions and efficient lysosomal delivery [36].
222 Finally, MTM1, a PI3P phosphatase, fine-tunes autophagosome maturation by modulating phospho-
223 inositide composition of autophagic membranes [16, 37, 38]. Dysregulation of MTM1 or related
224 myotubularins perturbs PI3P homeostasis and can compromise autophagosome–lysosome fusion, a
225 critical step for degradation.

226 Together, these findings underscore the tightly coordinated nature of autophagy regulation in KIRC.
227 Energy sensing by PRKAA2 and lipid transfer via VPS13D promote autophagy initiation, while
228 PIK3CA-driven mTOR activation imposes a strong inhibitory checkpoint. SNX30 and MTM1
229 ensure proper trafficking and maturation, linking vesicle dynamics to degradative capacity. The
230 convergence of these molecular alterations suggests that autophagy in KIRC is not simply switched
231 on or off, but instead dynamically rewired to balance metabolic needs, stress adaptation, and tumor
232 survival. Targeting this balance—through dual modulation of PI3K/AKT/mTOR signaling and
233 AMPK–autophagy activation—may represent a rational therapeutic strategy to exploit autophagy’s
234 context-dependent roles in renal cancer.

235 3.3 Catabolic Process Regulation as a Biomarker Signature in KIRC

236 Our analysis identified a significant enrichment of genes involved in the negative regulation of
237 catabolic processes (GO:0009895), including TIMP3, RGP1, OPHN1, and MTM1, which collectively
238 represent a metabolically relevant biomarker signature in kidney renal clear cell carcinoma (KIRC).
239 This finding aligns with the emerging understanding that dysregulated cellular catabolism is a hallmark
240 of renal cancer progression and therapeutic resistance.

241 TIMP3, the most clinically characterized gene in this pathway, functions as a critical gatekeeper of
242 extracellular matrix homeostasis by inhibiting matrix metalloproteinases that drive tumor invasion
243 and metastasis [39, 17]. In KIRC, TIMP3 downregulation has been associated with increased
244 invasive capacity and poor prognosis, suggesting its potential as both a prognostic biomarker and
245 therapeutic target [18]. The disruption of TIMP3-mediated negative regulation allows for enhanced
246 ECM degradation, facilitating the aggressive phenotype characteristic of advanced KIRC.

247 The inclusion of MTM1 and OPHN1 in this signature highlights the importance of membrane
248 dynamics and vesicular trafficking in cancer cell metabolism. MTM1’s role as a phosphoinositide
249 phosphatase places it at the intersection of autophagy regulation and metabolic reprogramming,
250 processes that are frequently dysregulated in renal cancers [19, 40]. Similarly, OPHN1’s involvement
251 in cytoskeletal remodeling and membrane trafficking suggests that the disruption of normal cellular
252 architectural control contributes to the catabolic dysregulation observed in KIRC.

253 The coordinated downregulation of these negative regulatory mechanisms may represent a fundamen-
254 tal shift toward a hyper-catabolic state that supports rapid tumor growth and adaptation to metabolic
255 stress. This is particularly relevant in KIRC, where metabolic reprogramming is a defining charac-
256 teristic, often driven by VHL gene alterations that affect cellular responses to hypoxia and nutrient
257 availability [41].

258 From a biomarker perspective, this catabolic regulation signature offers several advantages for
259 KIRC management. First, it provides insight into the metabolic state of tumors, which could
260 inform treatment selection, particularly for therapies targeting metabolic vulnerabilities. Second, the
261 coordinated expression of these genes may offer more robust prognostic information than individual
262 biomarkers alone. Finally, the pathway-level understanding of catabolic dysregulation could guide
263 the development of combination therapies that simultaneously target multiple nodes in this regulatory
264 network.

265 4 Conclusion

266 In summary, our integrative analysis of KIRC transcriptomes revealed a 76-gene signature that
267 defines two molecular subtypes with distinct prognostic outcomes. Differential expression and
268 survival analyses identified robust biomarker candidates, while enrichment analyses implicated
269 dysregulation of TOR signaling, autophagy, and catabolic processes as key drivers of disease pro-
270 gression. These findings not only advance the molecular understanding of KIRC but also provide
271 a refined biomarker framework for patient stratification and highlight pathway-level vulnerabilities
272 with potential therapeutic relevance.

273 **Broader impacts**

274 This study contributes to precision oncology by identifying molecular subtypes and prognostic
275 biomarkers in kidney renal clear cell carcinoma (KIRC) through integrative transcriptomic analysis.
276 The refined biomarker framework has the potential to improve patient stratification, guide treatment
277 selection, and uncover pathway-level vulnerabilities for therapeutic development. More broadly, the
278 methodological pipeline—combining survival-guided feature selection, clustering, and enrichment
279 analyses—can be generalized to other cancers and complex diseases, offering a scalable approach
280 for biomarker discovery and accelerating the integration of AI-assisted research into translational
281 medicine.

282 At the same time, both societal benefits and risks must be considered. Biomarker-driven models may
283 inadvertently exacerbate inequities if molecular profiling technologies are not equitably accessible.
284 Overreliance on computational outputs without rigorous clinical validation could also lead to prema-
285 ture or inappropriate application in patient care. In addition, the integration of AI into hypothesis
286 generation, experiment design, and manuscript drafting introduces concerns regarding transparency,
287 reproducibility, and authorship attribution.

288 To mitigate these risks, precautions were taken to ensure the safe deployment of the AI scientist.
289 All AI-generated hypotheses, analyses, and interpretations were reviewed and validated by human
290 researchers, with final responsibility for methodological rigor and scientific accuracy resting with
291 domain experts. Code, results, and textual outputs were cross-checked against established literature
292 and statistical standards to reduce the risk of erroneous conclusions. Clear documentation of the
293 AI's role in different stages of the research process has been provided to promote transparency and
294 accountability.

295 Overall, this work highlights the promise of AI-augmented biomedical discovery while emphasizing
296 the need for careful oversight, equitable access, and responsible integration to maximize societal
297 benefit and minimize harm.

298 **References**

- 299 [1] Jiajia Ma, Yuchu Xiang, Yan Liu, Xudong Liu, Xiaoting Pan, Lang Peng, and Bo Wang. Advances in
300 immunotherapy and targeted therapy for advanced clear-cell renal cell carcinoma: Current strategies and
301 future directions. *Frontiers in Immunology*, 16:1582887, 2025.
- 302 [2] Jacek Rysz, Janusz Ławiński, Beata Franczyk, and Anna Gluba-Sagr. Immune checkpoint inhibitors in
303 clear cell renal cell carcinoma (ccrcc). *International Journal of Molecular Sciences*, 26(12):5577, 2025.
- 304 [3] Yifan Zhang, Shengli Zhang, Hongbin Sun, and Luwei Xu. The pathogenesis and therapeutic implications
305 of metabolic reprogramming in renal cell carcinoma. *Cell Death Discovery*, 11(1):186, 2025.
- 306 [4] Filippo Gavi, Maria Chiara Sighinolfi, Giuseppe Pallotta, Simone Assumma, Enrico Panio, Daniele
307 Fettucciarri, Antonio Silvestri, Pierluigi Russo, Riccardo Bientinesi, Nazario Foschi, et al. Multiomics in
308 renal cell carcinoma: Current landscape and future directions for precision medicine. *Current Urology
Reports*, 26(1):44, 2025.
- 310 [5] Zhouzhou Xie, Shansen Peng, Jiongming Wang, Yueling Huang, Xiaoqi Zhou, Guihao Zhang, Huiming
311 Jiang, Kaihua Zhong, Lingsong Feng, and Nanhui Chen. Multi-omics analysis reveals the role of ribosome
312 biogenesis in malignant clear cell renal cell carcinoma and the development of a machine learning-based
313 prognostic model. *Frontiers in Immunology*, 16:1602898, 2025.
- 314 [6] Man Wang, Yuanzhuo Zhao, Kangchun Xu, Chao Liu, Hui Zhong, You Wu, Ke Zhang, and Shanzhai
315 Wei. Cancer-associated fibroblasts in clear cell renal cell carcinoma: functional heterogeneity, tumor
316 microenvironment crosstalk, and therapeutic opportunities. *Frontiers in Immunology*, 16:1617968, 2025.
- 317 [7] Yuntao Yao, Yifan Liu, Bingnan Lu, Guo Ji, Lei Wang, Keqin Dong, Zihui Zhao, Donghao Lyu, Maodong
318 Wei, Siqi Tu, et al. Construction and validation of a regulatory t cells-based classification of renal cell
319 carcinoma: an integrated bioinformatic analysis and clinical cohort study. *Cellular Oncology*, pages 1–25,
320 2024.
- 321 [8] Antoine Deleuze, Judikaël Saout, Frédéric Dugay, Benoit Peyronnet, Romain Mathieu, Gregory Verhoest,
322 Karim Bensalah, Laurence Crouzet, Brigitte Laguerre, Marc-Antoine Belaud-Rotureau, et al. Immunother-
323 apy in renal cell carcinoma: the future is now. *International Journal of Molecular Sciences*, 21(7):2532,
324 2020.

- 325 [9] Goncalo Outeiro-Pinho, Daniela Barros-Silva, Margareta P Correia, Rui Henrique, and Carmen Jeronimo.
326 Renal cell tumors: uncovering the biomarker potential of nernas. *Cancers*, 12(8):2214, 2020.
- 327 [10] Iseult M. Browne and Alicia F. C. Okines. Resistance to targeted inhibitors of the pi3k/akt/mTOR pathway
328 in advanced oestrogen-receptor-positive breast cancer. *Cancers*, 16(12), 2024. ISSN 2072-6694. doi:
329 10.3390/cancers16122259. URL <https://www.mdpi.com/2072-6694/16/12/2259>.
- 330 [11] Christos Gkogkas, Arkady Khoutorsky, Inbal Ran, et al. Autism-related deficits via dysregulated eif4e-
331 dependent translational control. *Nature*, 493(7432):371–377, 2013. doi: 10.1038/nature11628. URL
332 <https://doi.org/10.1038/nature11628>.
- 333 [12] Shraddha S. Mohanty, Shweta Warrier, and Annapoorni Rangarajan. Rethinking AMPK: A reversible switch
334 fortifying cancer cell stress-resilience. *The Yale Journal of Biology and Medicine*, 98(1):33–52, March
335 2025. ISSN 0044-0086. doi: 10.59249/JKBB6336. Epub 2025 Mar 31.
- 336 [13] A. Simon, N. Diedhiou, D. Reiss, et al. Potential compensatory mechanisms preserving cardiac func-
337 tion in myotubular myopathy. *Cellular and Molecular Life Sciences*, 81:476, 2024. doi: 10.1007/
338 s00018-024-05512-9. URL <https://doi.org/10.1007/s00018-024-05512-9>.
- 339 [14] Mingyang Jiang, Ke Zhang, Zhenwang Zhang, Xinran Zeng, Zihang Huang, Peizhuo Qin, Zhilin Xie, Xue
340 Cai, Milad Ashrafizadeh, Yu Tian, et al. PI3K/Akt/mTOR axis in cancer: from pathogenesis to treatment.
341 *MedComm*, 6(8):e70295, 2025.
- 342 [15] Samantha K Dziurdzik, Björn DM Bean, Michael Davey, and Elizabeth Conibear. A VPS13D spastic ataxia
343 mutation disrupts the conserved adaptor-binding site in yeast VPS13. *Human Molecular Genetics*, 29(4):
344 635–648, 2020.
- 345 [16] Bishal Basak and Erika LF Holzbaur. Mitochondrial damage triggers the concerted degradation of negative
346 regulators of neuronal autophagy. *Nature Communications*, 16(1):7367, 2025.
- 347 [17] B. Jeremiasse, C. Matta, C. R. Fellows, et al. Alterations in the chondrocyte surfaceome in re-
348 sponse to pro-inflammatory cytokines. *BMC Molecular and Cell Biology*, 21:47, 2020. doi: 10.1186/
349 s12860-020-00288-9. URL <https://doi.org/10.1186/s12860-020-00288-9>.
- 350 [18] N. White, H. Khella, J. Grigull, et al. miRNA profiling in metastatic renal cell carcinoma reveals a tumour-
351 suppressor effect for miR-215. *British Journal of Cancer*, 105:1741–1749, 2011. doi: 10.1038/bjc.2011.401.
352 URL <https://doi.org/10.1038/bjc.2011.401>.
- 353 [19] Yvonne Bouter, Tim Kacprowski, Fanny Rößler, Lars R. Jensen, Andreas W. Kuss, and Thomas A. Bayer.
354 miRNA alterations elicit pathways involved in memory decline and synaptic function in the hippocampus of
355 aged tg4-42 mice. *Frontiers in Neuroscience*, 14:580524, September 2020. doi: 10.3389/fnins.2020.580524.
356 URL <https://doi.org/10.3389/fnins.2020.580524>. Section: Neurodegeneration. Research Topic:
357 Deciphering the biomarkers of Alzheimer’s disease.
- 358 [20] Ziying Huang, Niaz Mahmood, Jean-Claude Lacaille, Shane Wiebe, and Nahum Sonenberg. Hippocampal
359 inhibitory interneuron-specific dREADDS treatment alters mTORC1-4e-BP signaling and impairs memory
360 formation. *Journal of Neurochemistry*, 169(3):e70048, 2025. doi: <https://doi.org/10.1111/jnc.70048>. URL
361 <https://onlinelibrary.wiley.com/doi/abs/10.1111/jnc.70048> e70048 JNC-2025-0025.R1.
- 362 [21] Y. Cui, J. Chen, Z. Zhang, et al. The role of AMPK in macrophage metabolism, function and polarisation.
363 *Journal of Translational Medicine*, 21(1):892, 2023. doi: 10.1186/s12967-023-04772-6. URL <https://doi.org/10.1186/s12967-023-04772-6>.
- 365 [22] W. S. Yang, S. H. Kim, M. Kim, et al. Structural basis for the recognition and ubiquitylation of type-2
366 n-degron substrate by PR1 plant n-recognin. *Nature Communications*, 16:7817, 2025. doi: 10.1038/
367 s41467-025-63282-9. URL <https://doi.org/10.1038/s41467-025-63282-9>.
- 368 [23] S. H. Kim, J. S. Park, M. H. Lee, et al. The n-degron pathway governs autophagy to promote thermotolerance
369 in Arabidopsis. *Nature Communications*, 16:5889, 2025. doi: 10.1038/s41467-025-61191-5. URL
370 <https://doi.org/10.1038/s41467-025-61191-5>.
- 371 [24] Mélanie Mansat, Afi Oportune Kpotor, Anne Mazars, Gaëtan Chicanne, Bernard Payrastre, and Julien
372 Viaud. PI3KC2β depletion rescues endosomal trafficking defects in *Mtm1* knockout skeletal muscle cells.
373 *Journal of Lipid Research*, 66(3):100756, 2025. ISSN 0022-2275. doi: 10.1016/j.jlr.2025.100756. URL
374 <https://doi.org/10.1016/j.jlr.2025.100756>.
- 375 [25] Jingru Wang, Na Fang, Juan Xiong, Yuanjiao Du, Yue Cao, and Wei-Ke Ji. An ESCRT-dependent step
376 in fatty acid transfer from lipid droplets to mitochondria through VPS13D-TSG101 interactions. *Nature
377 communications*, 12(1):1252, 2021.

- 378 [26] Xiaomeng Yin, Ruoxi Wang, Andrea Thackeray, Eric H Baehrecke, and Mark J Alkema. Vps13d mutations
379 affect mitochondrial homeostasis and locomotion in *caenorhabditis elegans*. *G3: Genes, Genomes,
380 Genetics*, 15(4):jkaf023, 2025.
- 381 [27] Shraddha S Mohanty, Shweta Warrier, and Annapoorni Rangarajan. Rethinking ampk: A reversible switch
382 fortifying cancer cell stress-resilience. *The Yale Journal of Biology and Medicine*, 98(1):33, 2025.
- 383 [28] Jiang Feng, Li MengHuan, Yao TingTing, Yi XueJie, and Gao HaiNing. Research progress on ampk in the
384 pathogenesis and treatment of masld. *Frontiers in Immunology*, 16:1558041, 2025.
- 385 [29] Francesca Zanieri, Ana Levi, David Montefusco, Lisa Longato, Francesco De Chiara, Luca Frenguelli, Sara
386 Omenetti, Fausto Andreola, Tu Vinh Luong, Veronica Massey, et al. Exogenous liposomal ceramide-c6
387 ameliorates lipidomic profile, energy homeostasis, and anti-oxidant systems in nash. *Cells*, 9(5):1237,
388 2020.
- 389 [30] Jeremi Laski, Bipradeb Singha, Xu Wang, Judith Ramos Valdés, Olga Collins, and Trevor G Shepherd.
390 Activated camkk β -ampk signaling promotes autophagy in a spheroid model of ovarian tumour metastasis.
391 *Journal of Ovarian Research*, 13(1):58, 2020.
- 392 [31] Hyemin Lee, Fereshteh Zandkarimi, Yilei Zhang, Jitendra Kumar Meena, Jongchan Kim, Li Zhuang,
393 Siddhartha Tyagi, Li Ma, Thomas F Westbrook, Gregory R Steinberg, et al. Energy-stress-mediated ampk
394 activation inhibits ferroptosis. *Nature cell biology*, 22(2):225–234, 2020.
- 395 [32] Ali Hassan and Corinne Aubel. The pi3k/akt/mTOR signaling pathway in triple-negative breast cancer: A
396 resistance pathway and a prime target for targeted therapies. *Cancers*, 17(13):2232, 2025.
- 397 [33] Jing Ma, Lu Ding, Xiaoyu Zang, Yingying Yang, Wei Zhang, Xiangyan Li, Daqing Zhao, Zepeng Zhang,
398 Zeyu Wang, Linhua Zhao, et al. Qimai feiluoping decoction inhibits endmt to alleviate pulmonary fibrosis
399 by reducing pi3k/akt/mTOR pathway-mediated the restoration of autophagy. *Journal of Inflammation
400 Research*, pages 8447–8475, 2025.
- 401 [34] Miguel A Ortega, Oscar Fraile-Martínez, Ángel Asúnsolo, Julia Buján, Natalio García-Hondurilla, and
402 Santiago Coca. Signal transduction pathways in breast cancer: the important role of pi3k/akt/mTOR. *Journal
403 of oncology*, 2020(1):9258396, 2020.
- 404 [35] Zhihang Chen, Chun Wang, Hao Dong, Xing Wang, Feng Gao, Sen Zhang, and Xiaolong Zhang. Aspirin
405 has a better effect on PIK3CA mutant colorectal cancer cells by PI3K/Akt/Raptor pathway. *Molecular Medicine*,
406 26(1):14, 2020.
- 407 [36] Johan-Owen De Craene, Dimitri L Bertazzi, Séverine Bär, and Sylvie Friant. Phosphoinositides, major
408 actors in membrane trafficking and lipid signaling pathways. *International journal of molecular sciences*,
409 18(3):634, 2017.
- 410 [37] Xiaokun Yu, Junfeng Ma, Feng Lin, Wanke Zhao, Xueqi Fu, and Zhizhuang Joe Zhao. Myotubularin
411 family phosphatase cemtm3 is required for muscle maintenance by preventing excessive autophagy in
412 *caenorhabditis elegans*. *BMC Cell Biology*, 13(1):28, 2012.
- 413 [38] Shun-ichi Yamashita, Masahide Oku, Yuko Wasada, Yoshitaka Ano, and Yasuyoshi Sakai. Pi4P-signaling
414 pathway for the synthesis of a nascent membrane structure in selective autophagy. *Journal of Cell
415 Biology*, 173(5):709–717, 06 2006. ISSN 0021-9525. doi: 10.1083/jcb.200512142. URL <https://doi.org/10.1083/jcb.200512142>.
- 416 [39] L. Baumgartner, S. Witta, and J. Noailly. Parallel networks to predict Timp and protease cell activity of
417 nucleus pulposus cells exposed and not exposed to pro-inflammatory cytokines. *JOR SPINE*, 8(1):e70051,
418 2025. doi: <https://doi.org/10.1002/jsp2.70051>. URL <https://onlinelibrary.wiley.com/doi/abs/10.1002/jsp2.70051>. e70051 JSP2-24-0272.R1.
- 419 [40] Ying Chen, Jinjun Qian, Pinggang Ding, Wang Wang, Xinying Li, Xiaozhu Tang, Chao Tang, Ye Yang,
420 and Chunyan Gu. Elevated sfxn2 limits mitochondrial autophagy and increases iron-mediated energy
421 production to promote multiple myeloma cell proliferation. *Cell Death & Disease*, 13:822, September
422 2022. doi: 10.1038/s41419-022-05256-6. URL <https://doi.org/10.1038/s41419-022-05256-6>.
- 423 [41] Shruti Gupta and Shamsher Singh Kanwar. Biomarkers in renal cell carcinoma and their targeted therapies:
424 a review. *Exploration of Targeted Anti-tumor Therapy*, 4:941–961, 2023. doi: 10.37349/etat.2023.00175.
425 URL <https://doi.org/10.37349/etat.2023.00175>. Special issue: Biomarkers for Personalized
426 and Precise Cancer Diagnosis and Treatment. Academic Editor: Arun Seth, University of Toronto, Canada.

429 **Agents4Science AI Involvement Checklist**

430 This checklist is designed to allow you to explain the role of AI in your research. This is important for
431 understanding broadly how researchers use AI and how this impacts the quality and characteristics
432 of the research. **Do not remove the checklist! Papers not including the checklist will be desk**
433 **rejected.** You will give a score for each of the categories that define the role of AI in each part of the
434 scientific process. The scores are as follows:

- 435 • **[A] Human-generated:** Humans generated 95% or more of the research, with AI being of
436 minimal involvement.
- 437 • **[B] Mostly human, assisted by AI:** The research was a collaboration between humans and
438 AI models, but humans produced the majority (>50%) of the research.
- 439 • **[C] Mostly AI, assisted by human:** The research task was a collaboration between humans
440 and AI models, but AI produced the majority (>50%) of the research.
- 441 • **[D] AI-generated:** AI performed over 95% of the research. This may involve minimal
442 human involvement, such as prompting or high-level guidance during the research process,
443 but the majority of the ideas and work came from the AI.

444 These categories leave room for interpretation, so we ask that the authors also include a brief
445 explanation elaborating on how AI was involved in the tasks for each category. Please keep your
446 explanation to less than 150 words.

- 447 1. **Hypothesis development:** Hypothesis development includes the process by which you
448 came to explore this research topic and research question. This can involve the background
449 research performed by either researchers or by AI. This can also involve whether the idea
450 was proposed by researchers or by AI.

451 Answer: **[C]**

452 Explanation: The overall research goal—biomarker discovery in KIRC using mRNA expres-
453 sion data—was set by the human researcher. Once this direction was given, the AI agent
454 generated hypotheses, explored possible stratification strategies, and refined the specific
455 research questions. Thus, the AI played a substantial but not initiating role in hypothesis
456 development.

- 457 2. **Experimental design and implementation:** This category includes design of experiments
458 that are used to test the hypotheses, coding and implementation of computational methods,
459 and the execution of these experiments.

460 Answer: **[D]**

461 Explanation: The AI agent was responsible for designing computational experiments, coding
462 the analysis pipeline, and implementing data processing and clustering methods. It generated
463 executable code and carried out the experiments without human coding input, meaning the
464 AI was fully responsible for this stage.

- 465 3. **Analysis of data and interpretation of results:** This category encompasses any process to
466 organize and process data for the experiments in the paper. It also includes interpretations of
467 the results of the study.

468 Answer: **[D]**

469 Explanation: The AI handled the complete analysis process: organizing raw mRNA data,
470 performing clustering and survival analyses, retrieving supporting literature, and interpreting
471 patterns in the results. It generated the summaries and interpretations that shaped the study's
472 findings. Human oversight was minimal at this stage.

- 473 4. **Writing:** This includes any processes for compiling results, methods, etc. into the final
474 paper form. This can involve not only writing of the main text but also figure-making,
475 improving layout of the manuscript, and formulation of narrative.

476 Answer: **[C]**

477 Explanation: The AI produced the draft content of all sections and generated figures, tables,
478 and narratives describing the results. The human researcher then compiled these outputs
479 into LaTeX, organized the manuscript structure, and finalized it for submission. This makes
480 the AI's role substantial but not fully independent.

481 **5. Observed AI Limitations:** What limitations have you found when using AI as a partner or
482 lead author?

483 Description: The AI agent occasionally demonstrates weaknesses in three key areas. First,
484 it may select or process data incorrectly due to limited awareness of the underlying data
485 structure. Second, it can misidentify or apply inappropriate software packages and analytic
486 tools for a given task. Third, the agent sometimes loses continuity across sequential
487 experimental steps, causing deviations from the initial objectives or inconsistencies with
488 earlier results.

489 **Agents4Science Paper Checklist**

490 The checklist is designed to encourage best practices for responsible machine learning research,
491 addressing issues of reproducibility, transparency, research ethics, and societal impact. Do not remove
492 the checklist: **Papers not including the checklist will be desk rejected.** The checklist should
493 follow the references and follow the (optional) supplemental material. The checklist does NOT count
494 towards the page limit.

495 Please read the checklist guidelines carefully for information on how to answer these questions. For
496 each question in the checklist:

- 497 • You should answer [Yes] , [No] , or [NA] .
498 • [NA] means either that the question is Not Applicable for that particular paper or the
499 relevant information is Not Available.
500 • Please provide a short (1–2 sentence) justification right after your answer (even for NA).

501 **The checklist answers are an integral part of your paper submission.** They are visible to the
502 reviewers and area chairs. You will be asked to also include it (after eventual revisions) with the final
503 version of your paper, and its final version will be published with the paper.

504 The reviewers of your paper will be asked to use the checklist as one of the factors in their evaluation.
505 While "[Yes]" is generally preferable to "[No]", it is perfectly acceptable to answer "[No]" provided
506 a proper justification is given. In general, answering "[No]" or "[NA]" is not grounds for rejection.
507 While the questions are phrased in a binary way, we acknowledge that the true answer is often more
508 nuanced, so please just use your best judgment and write a justification to elaborate. All supporting
509 evidence can appear either in the main paper or the supplemental material, provided in appendix.
510 If you answer [Yes] to a question, in the justification please point to the section(s) where related
511 material for the question can be found.

512 **1. Claims**

513 Question: Do the main claims made in the abstract and introduction accurately reflect the
514 paper's contributions and scope?

515 Answer: [Yes]

516 Justification: N/A

517 Guidelines:

- 518 • The answer NA means that the abstract and introduction do not include the claims
519 made in the paper.
520 • The abstract and/or introduction should clearly state the claims made, including the
521 contributions made in the paper and important assumptions and limitations. A No or
522 NA answer to this question will not be perceived well by the reviewers.
523 • The claims made should match theoretical and experimental results, and reflect how
524 much the results can be expected to generalize to other settings.
525 • It is fine to include aspirational goals as motivation as long as it is clear that these goals
526 are not attained by the paper.

527 **2. Limitations**

528 Question: Does the paper discuss the limitations of the work performed by the authors?

529 Answer: [Yes]

530 Justification: N/A

531 Guidelines:

- 532 • The answer NA means that the paper has no limitation while the answer No means that
533 the paper has limitations, but those are not discussed in the paper.
534 • The authors are encouraged to create a separate "Limitations" section in their paper.
535 • The paper should point out any strong assumptions and how robust the results are to
536 violations of these assumptions (e.g., independence assumptions, noiseless settings,
537 model well-specification, asymptotic approximations only holding locally). The authors

538 should reflect on how these assumptions might be violated in practice and what the
539 implications would be.

- 540 • The authors should reflect on the scope of the claims made, e.g., if the approach was
541 only tested on a few datasets or with a few runs. In general, empirical results often
542 depend on implicit assumptions, which should be articulated.
543 • The authors should reflect on the factors that influence the performance of the approach.
544 For example, a facial recognition algorithm may perform poorly when image resolution
545 is low or images are taken in low lighting.
546 • The authors should discuss the computational efficiency of the proposed algorithms
547 and how they scale with dataset size.
548 • If applicable, the authors should discuss possible limitations of their approach to
549 address problems of privacy and fairness.
550 • While the authors might fear that complete honesty about limitations might be used by
551 reviewers as grounds for rejection, a worse outcome might be that reviewers discover
552 limitations that aren't acknowledged in the paper. Reviewers will be specifically
553 instructed to not penalize honesty concerning limitations.

554 3. Theory assumptions and proofs

555 Question: For each theoretical result, does the paper provide the full set of assumptions and
556 a complete (and correct) proof?

557 Answer: [NA]

558 Justification: No theory was proposed in this paper.

559 Guidelines:

- 560 • The answer NA means that the paper does not include theoretical results.
561 • All the theorems, formulas, and proofs in the paper should be numbered and cross-
562 referenced.
563 • All assumptions should be clearly stated or referenced in the statement of any theorems.
564 • The proofs can either appear in the main paper or the supplemental material, but if
565 they appear in the supplemental material, the authors are encouraged to provide a short
566 proof sketch to provide intuition.

567 4. Experimental result reproducibility

568 Question: Does the paper fully disclose all the information needed to reproduce the main ex-
569 perimental results of the paper to the extent that it affects the main claims and/or conclusions
570 of the paper (regardless of whether the code and data are provided or not)?

571 Answer: [Yes]

572 Justification: N/A

573 Guidelines:

- 574 • The answer NA means that the paper does not include experiments.
575 • If the paper includes experiments, a No answer to this question will not be perceived
576 well by the reviewers: Making the paper reproducible is important.
577 • If the contribution is a dataset and/or model, the authors should describe the steps taken
578 to make their results reproducible or verifiable.
579 • We recognize that reproducibility may be tricky in some cases, in which case authors
580 are welcome to describe the particular way they provide for reproducibility. In the case
581 of closed-source models, it may be that access to the model is limited in some way
582 (e.g., to registered users), but it should be possible for other researchers to have some
583 path to reproducing or verifying the results.

584 5. Open access to data and code

585 Question: Does the paper provide open access to the data and code, with sufficient instruc-
586 tions to faithfully reproduce the main experimental results, as described in supplemental
587 material?

588 Answer: [Yes]

589 Justification: N/A

590 Guidelines:

- 591 • The answer NA means that paper does not include experiments requiring code.
- 592 • Please see the Agents4Science code and data submission guidelines on the conference
- 593 website for more details.
- 594 • While we encourage the release of code and data, we understand that this might not be
- 595 possible, so “No” is an acceptable answer. Papers cannot be rejected simply for not
- 596 including code, unless this is central to the contribution (e.g., for a new open-source
- 597 benchmark).
- 598 • The instructions should contain the exact command and environment needed to run to
- 599 reproduce the results.
- 600 • At submission time, to preserve anonymity, the authors should release anonymized
- 601 versions (if applicable).

602 **6. Experimental setting/details**

603 Question: Does the paper specify all the training and test details (e.g., data splits, hyper-

604 parameters, how they were chosen, type of optimizer, etc.) necessary to understand the

605 results?

606 Answer: [Yes]

607 Justification: N/A

608 Guidelines:

- 609 • The answer NA means that the paper does not include experiments.
- 610 • The experimental setting should be presented in the core of the paper to a level of detail
- 611 that is necessary to appreciate the results and make sense of them.
- 612 • The full details can be provided either with the code, in appendix, or as supplemental
- 613 material.

614 **7. Experiment statistical significance**

615 Question: Does the paper report error bars suitably and correctly defined or other appropriate

616 information about the statistical significance of the experiments?

617 Answer: [Yes]

618 Justification: N/A

619 Guidelines:

- 620 • The answer NA means that the paper does not include experiments.
- 621 • The authors should answer "Yes" if the results are accompanied by error bars, confi-
- 622 dence intervals, or statistical significance tests, at least for the experiments that support
- 623 the main claims of the paper.
- 624 • The factors of variability that the error bars are capturing should be clearly stated
- 625 (for example, train/test split, initialization, or overall run with given experimental
- 626 conditions).

627 **8. Experiments compute resources**

628 Question: For each experiment, does the paper provide sufficient information on the com-

629 puter resources (type of compute workers, memory, time of execution) needed to reproduce

630 the experiments?

631 Answer: [NA]

632 Justification: N/A

633 Guidelines:

- 634 • The answer NA means that the paper does not include experiments.
- 635 • The paper should indicate the type of compute workers CPU or GPU, internal cluster,
- 636 or cloud provider, including relevant memory and storage.
- 637 • The paper should provide the amount of compute required for each of the individual
- 638 experimental runs as well as estimate the total compute.

639 **9. Code of ethics**

640 Question: Does the research conducted in the paper conform, in every respect, with the
641 Agents4Science Code of Ethics (see conference website)?

642 Answer: [Yes]

643 Justification: N/A

644 Guidelines:

- 645 • The answer NA means that the authors have not reviewed the Agents4Science Code of
646 Ethics.
- 647 • If the authors answer No, they should explain the special circumstances that require a
648 deviation from the Code of Ethics.

649 10. Broader impacts

650 Question: Does the paper discuss both potential positive societal impacts and negative
651 societal impacts of the work performed?

652 Answer: [Yes]

653 Justification: N/A

654 Guidelines:

- 655 • The answer NA means that there is no societal impact of the work performed.
- 656 • If the authors answer NA or No, they should explain why their work has no societal
657 impact or why the paper does not address societal impact.
- 658 • Examples of negative societal impacts include potential malicious or unintended uses
659 (e.g., disinformation, generating fake profiles, surveillance), fairness considerations,
660 privacy considerations, and security considerations.
- 661 • If there are negative societal impacts, the authors could also discuss possible mitigation
662 strategies.